International Journal of Thermophysics, Vol. 17, No. 4, 1996

Transport Properties of 1,1-Difluoroethane (R152a)

R. Krauss,[1] V. C. Weiss,[2,3] T. A. Edison,[2,4] J. V. Sengers,[2,4,5] and K. Stephan[1]

Received August 18, 1995

Based on reliable, carefully selected data sets, equations for the thermal conductivity and the viscosity of the refrigerant R152a are presented. They are valid at temperatures from 240 to 440 K, pressures up to 20 MPa, and densities up to 1050 $kg \cdot m^{-3}$, including the critical region.

KEY WORDS: 1,1-difluoroethane; correlation; critical region; HFC-152a; R152a; thermal conductivity; transport properties; viscosity.

1. INTRODUCTION

1,1-Difluoroethane (R152a) is one of the most promising long-term replacement refrigerants for chlorofluorocarbons (CFCs), whose production is to be phased out by 1996 according to the Montréal protocol. R152a combines a zero ozone-depletion potential (ODP) and a comparatively low global-warming potential of 150 (relative to CO_2 for a 100-year integration time horizon) [1] with other properties desirable for refrigerants such as a low toxicity, chemical stability, and compatibility with lubricant oils, the only disadvantage being its flammability. For this reason it is used as a component of binary or ternary mixtures of HFCs. This application implies a demand for reliable expressions for the transport properties of R152a.

[1] Universität Stuttgart, Institut für Technische Thermodynamik und Thermische Verfahrenstechnik, 70550 Stuttgart, Germany.
[2] Institute for Physical Science and Technology, University of Maryland, College Park, Maryland 20742, U.S.A.
[3] Universität Bremen, Fachbereich 2—Chemie, NW II, Leobener Strasse, 28359 Bremen, Germany.
[4] Department of Chemical Engineering and Center for Environmental Energy Engineering, University of Maryland, College Park, Maryland 20742, U.S.A.
[5] To whom correspondence should be addressed.

0195-928X/96/0700-0731$09.50/0

A preliminary evaluation and correlation of the transport properties, which omitted critical enhancements, was published by two of the present authors [2, 3]. However, in practice the thermal conductivity exhibits a pronounced critical enhancement in a large range of temperatures and densities [4, 5]. An equation for the thermodynamic properties of R152a in the critical region has recently been developed by van Pelt and Sengers [6] as a supplement to a global equation for the thermodynamic properties of R152a provided by Tillner-Roth [7]. Hence, it is now possible to present equations for the transport properties of R152a over an appreciable range of temperatures and densities including the critical region.

2. METHODOLOGY

In the present evaluation and correlation of the viscosity and thermal conductivity of R152a we apply the residual concept following the evaluation and correlation scheme outlined in detail in previous publications [8–11]. That is, within the uncertainty of the measurements, the viscosity $\eta(\rho, T)$ and the thermal conductivity $\lambda(\rho, T)$, respectively, as a function of density ρ and temperature T may be represented as the sum of three contributions:

$$\eta(\rho, T) = \eta_0(T) + \Delta_R\eta(\rho) + \Delta_c\eta(\rho, T) \tag{1}$$

$$\lambda(\rho, T) = \lambda_0(T) + \Delta_R\lambda(\rho) + \Delta_c\lambda(\rho, T) \tag{2}$$

The dilute-gas contributions $\eta_0(T)$ and $\lambda_0(T)$ depend only on the temperature. They can be treated independently from the other contributions. The excess terms $\Delta_R\eta(\rho)$ and $\Delta_R\lambda(\rho)$ account for the pressure or density dependence in the absence of critical fluctuations. As was the case for R134a [9], we neglect any temperature dependence of the excess terms because the resulting errors in the transport properties in the temperature range investigated are smaller than the experimental uncertainties. The dilute-gas and the excess terms together represent the so-called backgrounds $\bar{\eta}$ and $\bar{\lambda}$ of the viscosity and thermal conductivity, respectively [4]. The remaining contributions $\Delta_c\eta(\rho, T)$ and $\Delta_c\lambda(\rho, T)$ represent the critical enhancement of the viscosity and thermal conductivity, respectively. As the critical enhancement of the viscosity is small and occurs only in the very close vicinity of the critical point [12] and since for R152a no viscosity measurements exist in this region, the available experimental data for R152a can be represented by the background viscosity $\eta(\rho, T) = \bar{\eta}(\rho, T) = \eta_0(T) + \Delta_R\eta(\rho)$. However, the critical enhancement of the thermal conductivity is very significant. In order to separate the excess term and the critical enhancement term of the thermal conductivity, both contributions have to be determined in an iterative process as described in detail by Vesovic et al. [8].

To convert experimental pressures P into densities ρ and to calculate the various thermodynamic properties needed for the evaluation of the critical enhancement contributions, we need an equation of state. For this purpose we have adapted a global equation of state developed by Tillner-Roth [7], far away from the critical point, and a crossover equation of state recently developed by van Pelt and Sengers [6], which incorporates the singular behavior of the thermodynamic properties near the critical point. Specifically, the equation of van Pelt and Sengers has been used in a range of temperatures T around the critical temperature bounded by [6]

$$365\ \mathrm{K} \leqslant T \leqslant T_c \left(\frac{3}{4} + \frac{3\rho}{4\rho_c} - \frac{\rho^2}{3\rho_c^2} \right) \tag{3}$$

where $T_c = 386.411$ K and $\rho_c = 368.0\ \mathrm{kg \cdot m^{-3}}$ are the critical temperature and critical density, respectively. Outside this range the equation of state of Tillner-Roth has been used. Temperatures in this paper are in terms of ITS 90.

Table I. Viscosity References—Comparison with Eq. (1)[a]

Ref. No.	First author	P (MPa)	T (K)	Phase	Method	AME/MAX	Points
13	Assael	1.5–18	273–333	l	VW	0.9/−2.6	32
13	Assael		273–333	sl	VW	0.7/2.0	7
14	Mayinger	0.1	248–433	v	OD	0.2/0.7	20
15	Takahashi	0.1–5.3	298–423	v	OD	0.8/−2.1	103
16	Takahashi	0.1–0.7	273–303	v	OD	0.6/−1.8	49
17	van der Gulik		243–373	sl	VW	0.9/2.4	35
18	Arnemann		243–352	sl	RB	3.4/10.1	12
19	Heide		233–333	sl	RB	4.0/−7.0	10
20	Kumagai		273–343	sl	CV	1.8/6.3	8
21	Kumagai		273–343	sl	CV	2.7/9.0	8
22	Lapardin	0.1–50	156–434	l, v	CV	7.3/−20	47
14	Mayinger	0.1–12	253–493	v	OD	2.1/20	209
14	Mayinger		249–386	sv	OD	5.9/34	12
23	Mears		243–333	sl	CV	40/63	8
24	Nagaoka	0.1	298–323	v	RB	0.7/1.7	2
25	Phillips		200–318	sl	CV	5.7/11	6
26	Sagaidakova		163–383	sl	C	1.2/−6.3	15
27	Schramm		233–600	dil	C	0.6/−0.9	8
28	Takahashi		294–386	sv	OD	3.0/−5.9	19
17	van der Gulik		243–373	sv	VW	8.0/27	36

[a] Phase: dil = dilute gas; l = liquid; v = vapor; s = saturated. Method: C = calculated; CV = capillary viscometer; OD = oscillating disk; RB = rolling ball; VW = vibrating wire. AME/MAX: absolute mean error (%)/maximum error (%). Points: number of points compared within the range of validity of the correlation.

3. BACKGROUND VISCOSITY

The viscosity of R152a has been measured mainly in the liquid region at saturation. Four pressure-dependent data sets are available in the vapor phase, and three at saturated-vapor states. No experimental data near the critical point have been reported. In Table I we list 16 references for the viscosity together with the total pressure and temperature ranges, the phase, the experimental method, and the deviation of each data set with respect to the present correlation. The references listed above the solid line were used for the correlation. The data analysis shows that more measurements are desirable, especially in the subcritical vapor phase and in the critical region.

3.1. Dilute-Gas Viscosity

The dilute-gas viscosity η_0 is represented by an expression derived from the kinetic theory of gases,

$$\eta_0 = \frac{5}{16}\sqrt{\frac{MkT}{\pi N_A}}\frac{10^{24}}{\sigma^2\Omega_\eta(T^*)} = \frac{0.2169614\sqrt{T}}{\sigma^2\Omega_\eta(T^*)} \tag{4}$$

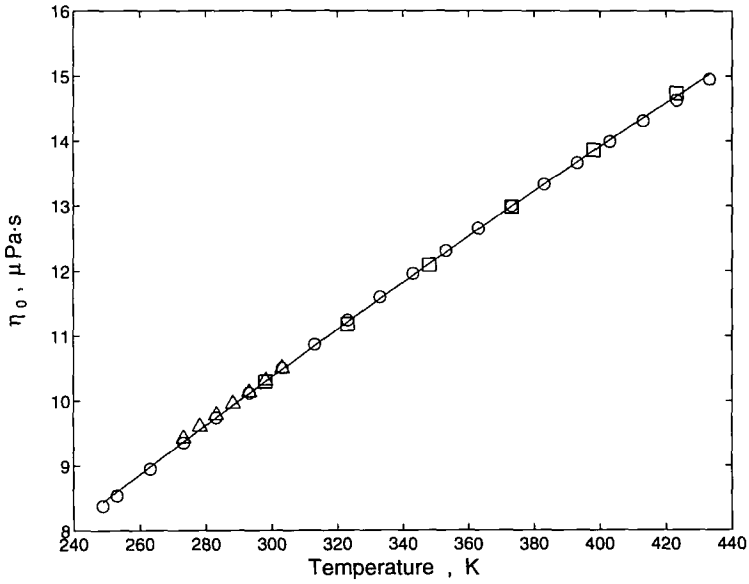

Fig. 1. The viscosity η_0 of R152a in the dilute-gas limit. The solid line represents the values calculated from Eq. (4); the data points shown are those reported by Takahashi et al. [15] (□), Takahashi et al. [16] (△), and Mayinger [14] (○).

where $M = 0.06605$ kg · mol^{-1} is the molecular mass, k is Boltzmann's constant in J · K^{-1}, N_A is Avogadro's number in mol^{-1}, and T is the temperature in K; η_0 obtained from this equation is in μPa · s. The collision integral is represented by an equation developed by Bich et al. [29],

$$\ln \Omega_\eta(T^*) = \sum_{i=0}^{4} A_i (\ln T^*)^i \tag{5}$$

with the reduced dimensionless temperature $T^* = kT/\varepsilon$ and the coefficients A_i listed in Table II. The energy scaling factor $\varepsilon/k = 354.84$ K and the length scaling factor $\sigma = 0.46115$ nm were estimated by fitting Eq. (4) to the experimental data reported by Takahashi et al. [15, 16] and Mayinger [14]. Figure 1 shows the equation for the dilute-gas viscosity as a solid line together with the above-mentioned data, which are indicated by symbols in the temperature range 240 to 440 K. The deviations are within $\pm 1\%$ as shown in Fig. 2.

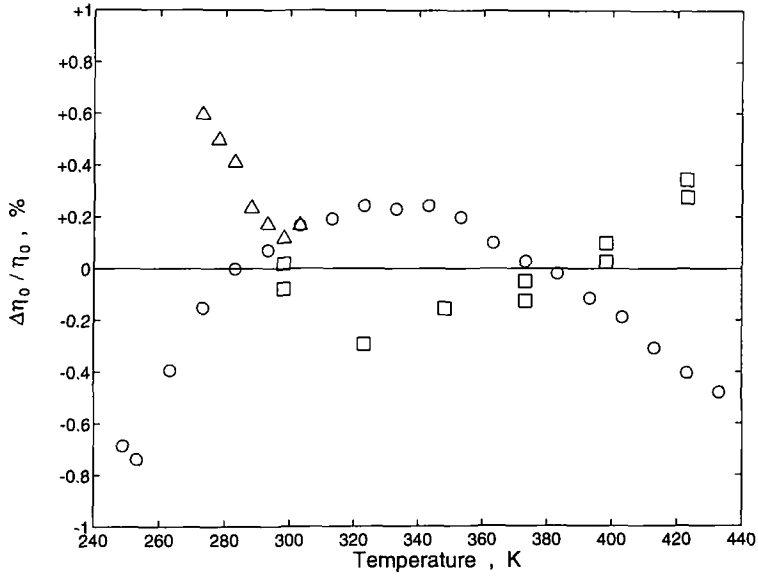

Fig. 2. Relative deviations (%) of the experimental viscosity data of Takahashi et al. [15] (□), Takahashi et al. [16] (△), and Mayinger [14] (○) from the corresponding values calculated with Eq. (4) for $\eta_0(T)$.

Table II. Coefficients in Eqs. (5) and (6)

i	A_i	E_i
0	0.4425728	—
1	−0.5138403	−0.0737927
2	0.1547566	0.517924
3	−0.02821844	−0.308875
4	0.001578286	0.108049
5	—	−0.408387
6	—	2.91733

3.2. Excess Viscosity

The dimensionless excess viscosity

$$\frac{\Delta_R \eta}{H_c} = \sum_{i=1}^{4} E_i \left(\frac{\rho}{\rho_c}\right)^i + \frac{E_5}{\rho/\rho_c - E_6} + \frac{E_5}{E_6} \tag{6}$$

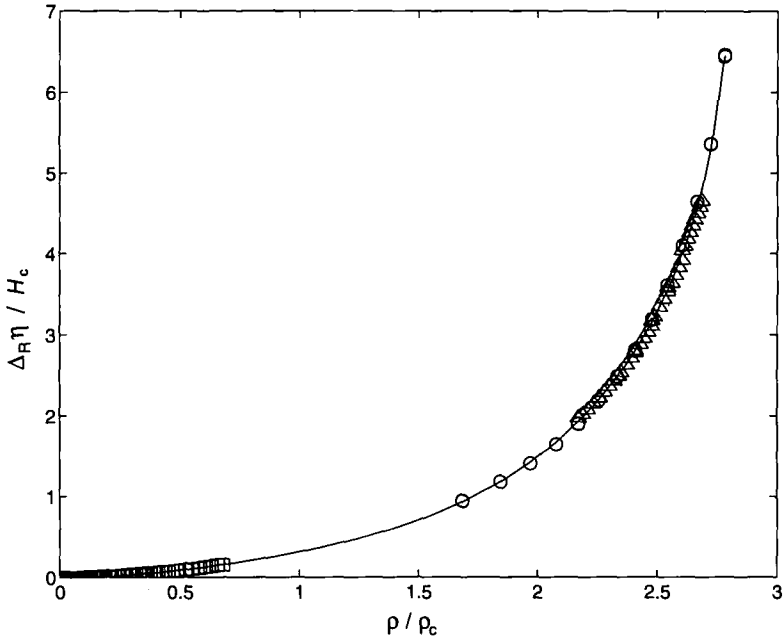

Fig. 3. The dimensionless excess contribution to the viscosity of R152a. The solid line represents the values calculated from Eq. (6); the data points shown are those reported by Takahashi et al. [15] (□), Assael *et al.* [13] (△), and van der Gulik [17] (○).

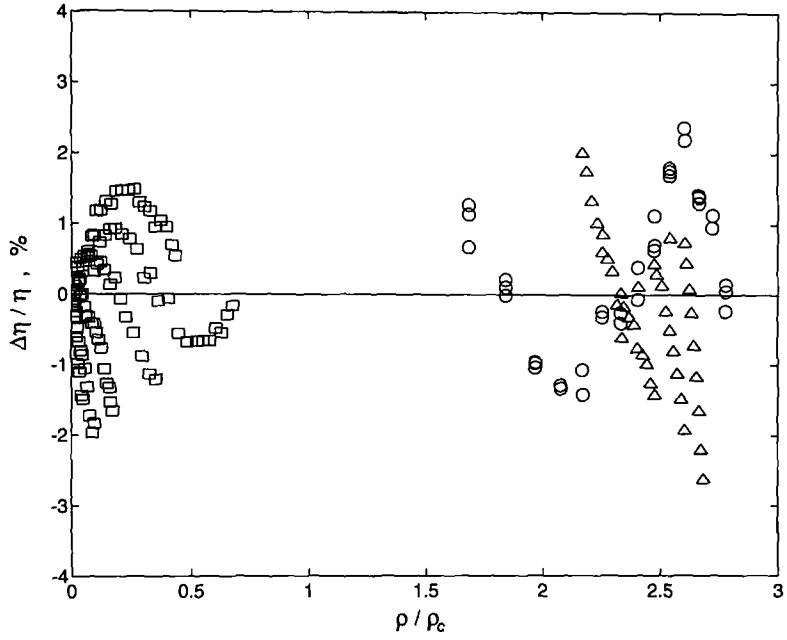

Fig. 4. Relative deviations (%) of the experimental viscosity data of Takahashi et al. [15] (□), Assael et al. [13] (△), and van der Gulik [17] (○) from the values calculated with Eqs. (4) and (6) for the background viscosity $\bar{\eta}$.

is represented by a fourth-order polynomial with a hyperbolic term accounting for the steep increase in the viscosity at high densities, where the viscosity reduction factor $H_c = 51.12\,\mu\text{Pa}\cdot\text{s}$ is a so-called pseudo-critical viscosity deduced from a dimensional analysis [9, 30]. The coefficients E_i in Eq. (6) are given in Table II. They were determined from a fit to the vapor-phase data of Takahashi et al. [15], revised saturated-liquid data of van der Gulik [17], and measurements of Assael et al. [13] as shown in Fig. 3. The equation represents the experimental data within ±3% from 240 to 440 K at pressures; up to 20 MPa and densities up to 1050 $\text{kg}\cdot\text{m}^{-3}$, as shown in Fig. 4.

4. BACKGROUND THERMAL CONDUCTIVITY

The available references for the thermal conductivity of R152a are listed in Table III. Most measurements were carried out in the liquid phase. Six data sets exist for the thermal conductivity at atmospheric pressure. The correlation is based on the data sets listed above the solid line. Additional measurements are needed mainly in the subcritical vapor phase, even at atmospheric pressure, and in the near and extended critical region.

Table III. Thermal Conductivity References—Comparison with Eq. (2)[a]

Ref. No.	First author	P (MPa)	T (K)	Phase	Method	AME/MAX	Points
31	Afshar		280–510	dil	HW	1.0/3.2	10
32	Assael	0.5–22	253–333	l	HW, T	0.8/1.5	37
32	Assael		253–333	sl	HW, T	0.6/1.1	5
33	Gurova	0.8–18	212–294	l	HW, T	1.5/−2.8	24
34	Hammerschmidt	0.1	303–463	v	PP	1.3/2.4	5
35	Kim	2.1–20	223–323	l	HW, T	0.5/2.1	20
35	Kim		223–323	sl	HW, T	1.1/2.6	4
36	Kraft		279–386	sl	DLS	1.3/3.2	15
37	Kruppa	0.5–11	293–426	l, v, sl	DLS	1.5/−4.3	27
38	Taxis-Reischl	0.1–2.4	277–400	v	HW, T	1.3/6.5	54
39	Tsvetkov	7.7–8.6	190–300	l	CC, T	2.2/2.8	6
40	Geller	0.1–6.9	305–433	l, v	HW, S	3.9/16	126
41	Grebenkov	1.0–20	294–341	l	CC	3.2/−7.1	78
42	Gross	0.1–6.2	253–313	l	HS	3.6/4.1	18
43	Gross	0.1–6.2	253–363	l, v, sl, sv	HW, T	3.5/26	111
19	Heide		233–333	sl	CC	4.6/5.5	10
44	Ibreighith		278–323	l	DLS	5.3/20	24
45	Kesselman		213–333	sl	HW, S	1.3/−2.6	10
36	Kraft		360–386	sv	DLS	3.1/4.2	6
46	Tauscher		163–298	sl	HW, T	3.4/3.6	7
47	Vargaftik	0.2–4	265–500	l, v	CO	2.9/10.5	41
48	Yata	1.4–31	265–343	l	HW, T	2.8/−6.0	20
49	Yin	0.1	279–349	v	HW, T	8.5/−11	14

[a] Phase: dil = dilute gas; l = liquid; v = vapor; s = saturated. Method: CC = coaxial cylinder; CO = compilation; DLS = dynamic light scattering; HS = hot strip; HW = hot wire (S = steady state; T = transient); PP = parallel plate. AME/MAX: absolute mean error (%)/maximum error (%). Points: number of points compared within the range of validity of the correlation.

4.1. Dilute-Gas Thermal Conductivity

The dilute-gas function for the thermal conductivity

$$\lambda_0 = B_0 + B_1 T \tag{7}$$

is represented by an empirical linear polynomial with λ_0 in $\mathrm{mW \cdot m^{-1} \cdot K^{-1}}$ and the temperature T in K [2, 3]. It is based on the data of Afshar and Saxena [31], Hammerschmidt [34], and Taxis-Reischl [38] as indicated in Fig. 5 in the temperature range 280 to 460 K, but extrapolation down to 240 K seems possible. The coefficients B_i in Eq. (7) are given in Table IV. Figure 6 shows that the uncertainty of the fit is about ±3%.

Table IV. Coefficients in Eqs. (7) and (8)

i	B_i	L_i
0	−14.9420	—
1	0.0973283	9.18090
2	—	11.8577
3	—	−5.44730
4	—	1.71379

4.2. Excess Thermal Conductivity

The dimensionless excess thermal conductivity is expressed as

$$\frac{\Delta_R \lambda}{\Lambda_c} = \sum_{i=1}^{4} L_i \left(\frac{\rho}{\rho_c}\right)^i \tag{8}$$

with the thermal-conductivity reduction factor $\Lambda_c = 1.155\ \mathrm{mW \cdot m^{-1} \cdot K^{-1}}$ deduced from a dimensional analysis [9, 30]. The coefficients L_i are listed in Table IV. The correlation of the excess data is based on the measurements

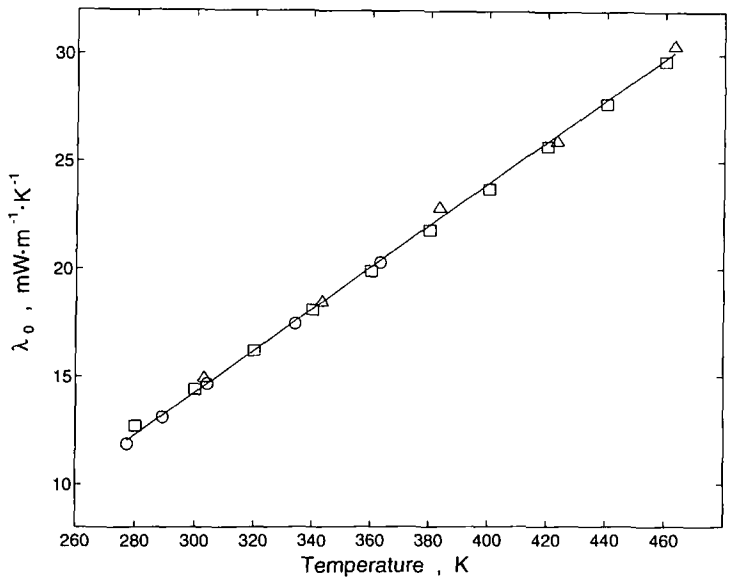

Fig. 5. The thermal conductivity λ_0 of R152a in the dilute-gas limit. The solid line represents the values calculated from Eq. (7); the data points shown are those reported by Afshar and Saxena [31] (□), Hammerschmidt [34] (△), and Taxis-Reischl [38] (○).

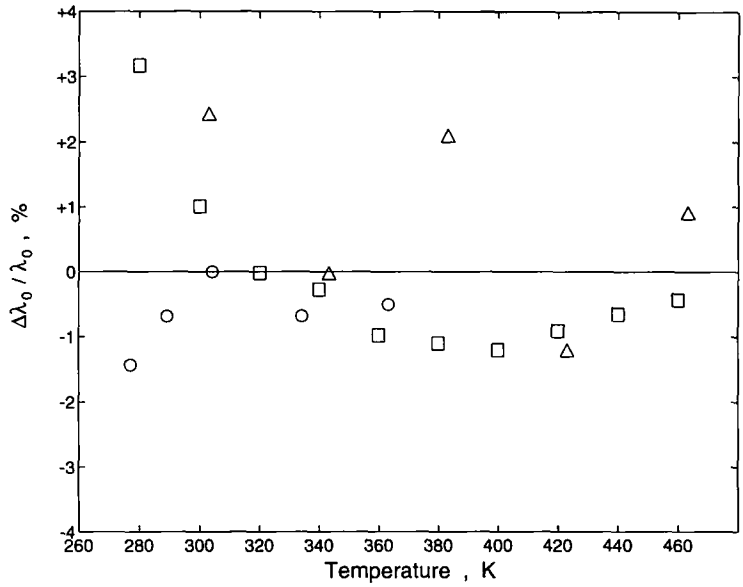

Fig. 6. Relative deviations (%) of the experimental thermal-conductivity data of Afshar and Saxena [31] (□), Hammerschmidt [34] (△), and Taxis-Reischl [38] (○) from the values calculated with Eq. (7) for $\lambda_0(T)$.

of Assael et al. [32], Gurova et al. [33], Kim et al. [35], and Tsvetkov et al. [39] in the liquid phase, the vapor-phase measurements of Taxis-Reischl [38], and the thermal-diffusivity measurements of Kruppa and Straub [37] as well as those of Kraft and Leipertz [36], as shown in Fig. 7. Equation (8) is valid in the temperature range 240 to 440 K, at pressures up to 20 MPa and densities up to 1050 $kg \cdot m^{-3}$. The deviation plot in Fig. 8 shows that the equation represents the thermal-conductivity data within $\pm 5\%$ in both the vapor and the liquid phase.

5. THE CRITICAL REGION

In Section 2, each of the transport properties was decomposed into three terms; the first two determine the background contributions $\bar{\eta}$ and $\bar{\lambda}$, while $\Delta_c\eta$ and $\Delta_c\lambda$ represent the increase in the transport properties due to critical fluctuations. The critical enhancements are represented by a theoretical crossover model originally developed by Olchowy and Sengers [12], which has been used previously to represent the transport properties of a variety of fluids in the critical region [8–11, 30, 50–55] and which recently has been slightly modified by Luettmer-Strathmann et al. [56, 57]

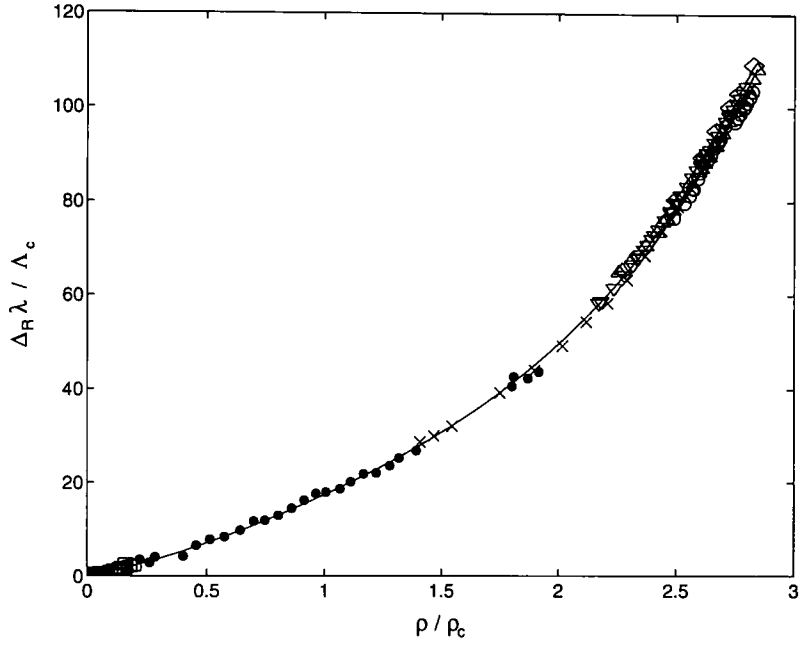

Fig. 7. The dimensionless excess contribution to the thermal conductivity of R152a. The solid line represents the values calculated from Eq. (8); the data points shown are those reported by Taxis-Reischl [38] (□), Kim et al. [35] (△), Assael et al. [32] (▽), Tsvetkov et al. [39] (◇), Gurova et al. [33] (○), Kruppa and Straub [37] (●), and Kraft and Leipertz [36] (×).

This crossover model is based on the mode-coupling theory for the dynamical behavior of critical fluctuations [56].

The thermal diffusivity D_T is related to the thermal conductivity λ as

$$D_T = \frac{\lambda}{\rho c_p} \tag{9}$$

where c_p is the isobaric specific heat capacity. The critical part $\Delta_c D_T$ of the thermal diffusivity is given by

$$\Delta_c D_T = \frac{\Delta_c \lambda}{\rho c_p} \tag{10}$$

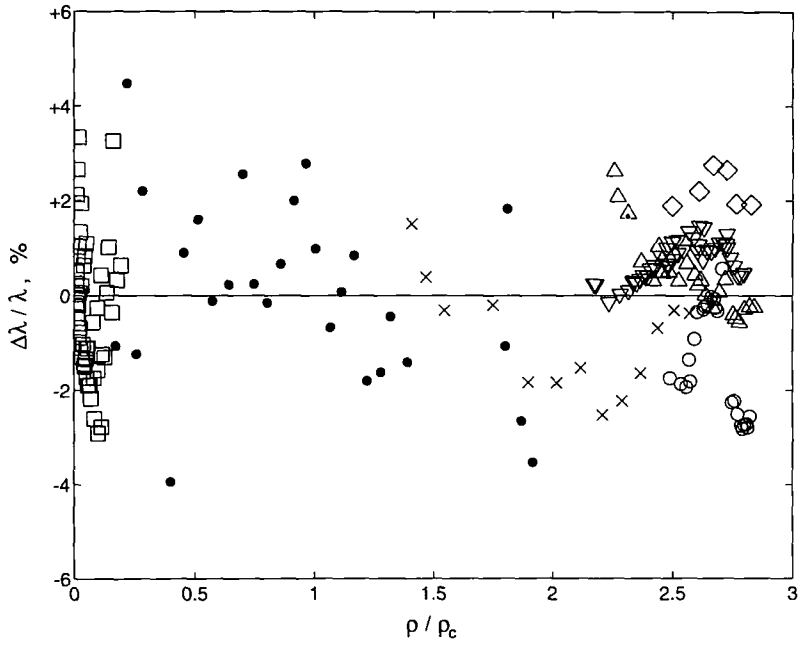

Fig. 8. Relative deviations (%) of the experimental thermal-conductivity data of Taxis-Reischl [38] (□), Kim et al. [35] (△), Assael et al. [32] (▽), Tsvetkov et al. [38] (◇), Gurova et al. [33] (○), Kruppa and Straub [37] (●), and Kraft and Leipertz [36] (×) from the values calculated with Eqs. (7) and (8) for the background thermal conductivity $\bar{\lambda}$.

Asymptotically close to the critical point $\Delta_c D_T$ satisfies a Stokes–Einstein relation of the form [4]

$$\Delta_c D_T = \frac{R_0 kT}{6\pi\eta\xi} \tag{11}$$

where k is Boltzmann's constant, ξ the correlation length of the critical fluctuations, and R_0 a universal amplitude for which we adopted a value of $R_0 = 1.03$ [9].

The viscosity exhibits a weak divergent critical enhancement of the form [4]

$$\Delta_c \eta = \bar{\eta}[(Q\xi)^z - 1] \tag{12}$$

where Q is a system-dependent amplitude and where $z = 0.063$ is a universal critical exponent [58–60].

In the crossover model these asymptotic expressions are generalized to

$$\Delta_c D_T = \frac{R_0 k T}{6\pi\eta\xi}(\Omega - \Omega_0) \tag{13}$$

$$\eta = \bar{\eta} e^{czH} \tag{14}$$

where $\Omega - \Omega_0$ and H are crossover functions that depend on the thermodynamic properties, on the correlation length ξ, and on the background transport properties $\bar{\lambda}$ and $\bar{\eta}$ and they contain one system-dependent parameter q_D, which represents a cutoff wavenumber of the critical fluctuations [50]. The coefficient c in expression (14) for η is given by [55].

$$c = \left(2 - \frac{\alpha + \gamma}{2\nu}\right)^{-1} = 1.075 \tag{15}$$

where $\alpha = 0.110$, $\gamma = 1.239$, and $\nu = 0.630$ are the critical exponents for the isochoric specific heat capacity c_v, the susceptibility $\chi = \rho(\partial\rho/\partial p)_T$, and the correlation length ξ, respectively [58]. Detailed expressions for the crossover functions Ω, Ω_0, and H have been presented in previous publications [50, 53]. For the present correlation we have used similar but slightly modified expressions as specified elsewhere [56, 57].

The crossover functions depend on the correlation length ξ, which for practical purposes is calculated from the dimensionless susceptibility

$$\chi^*(T, \rho) = \frac{\rho P_c}{\rho_c^2}\left(\frac{\partial\rho}{\partial P}\right)_T \tag{16}$$

where $P_c = 4.520$ MPa is the critical pressure, through an equation of the form [9]

$$\xi = \xi_0 \left[\frac{1}{\Gamma}\left(\chi^*(T, \rho) - \chi^*(T_{ref}, \rho)\frac{T_{ref}}{T}\right)\right]^{\nu/\gamma} \tag{17}$$

Here $\xi_0 = 1.894 \times 10^{-10}$ m and $\Gamma = 0.0487$ are the amplitudes of the critical power laws for ξ and χ^* [58] and whose values can be deduced from the asymptotic behavior of the equation of state [6]. T_{ref} is a reference temperature which is chosen in such a way that the critical enhancement of the thermal conductivity $\Delta_c\lambda$ is negligibly small for temperatures greater than T_{ref}; we continued to choose $T_{ref} = \frac{3}{2}T_c$ as previously adapted for R134a [9]. The cutoff wavenumber q_D was treated as an adjustable constant to be determined from a fit to experimental thermal-diffusivity data [37]. The values of all constants that appear in the equations (13) for

Table V. Constants in the Equations for the Critical Enhancements $\Delta_c\eta$ and $\Delta_c\lambda$

Critical parameters
$T_c = 386.411$ K
$\rho_c = 368.0\ \text{kg} \cdot \text{m}^{-3}$
$P_c = 4.520$ MPa
Universal constants
$R_0 = 1.03$
$z = 0.063$
$\gamma = 1.239$
$\nu = 0.63$
$\alpha = 0.110$
Critical amplitudes
$\Gamma = 0.0487$
$\xi_0 = 1.894 \times 10^{-10}$ m
Reference temperature
$T_{\text{ref}} = \frac{3}{2}T_c$
Cutoff wavenumber
$q_D^{-1} = 4.37 \times 10^{-10}$ m

$\Delta_c D_T$ and (14) for $\eta/\bar{\eta}$ are listed in Table V. The critical enhancement $\Delta_c\lambda$ of the thermal conductivity is deduced from $\Delta_c D_T$ through Eq. (10). The various thermodynamic properties in the crossover model were calculated from the equations of state of van Pelt and Sengers [6] and of Tillner-Roth [7] as specified in Section 2.

Thermal-diffusivity data deduced from dynamic light-scattering measurements have been obtained by Kraft and Leipertz [36] and by Kruppa and Straub [37] for R152a in the critical region. Kruppa and Straub obtained 300 data points along seven isotherms on the liquid and vapor sides of the phase boundary, as well as along the critical isochore. Kraft and Leipertz have reported 22 data points along the liquid and vapor sides of the phase boundary.

Kruppa and Straub found a critical temperature of $T_c = 386.442$ K (ITS90) from their data. Since we used a value of $T_c = 386.411$ K [6], we shifted their temperatures by -0.031 K. Furthermore, they quote a critical density of $\rho_c = 368\ \text{kg} \cdot \text{m}^{-3}$ taken from the literature [62] for their calculations, but the thermal-diffusivity data for the lowest supercritical isotherm show that ρ_c might be slightly larger. Therefore, we adopted a value of $\rho_c = 369.5\ \text{kg} \cdot \text{m}^{-3}$ for their data and recalculated their densities according to this assumption.

In the absence of actual measurements of the thermal conductivity λ in the critical region, we instead calculated λ from the experimental thermal diffusivity D_T as

$$\lambda = \rho c_p D_T \tag{18}$$

The uncertainty in the thermal conductivity data obtained according to the above equation can be calculated in the following way: Kruppa and Straub claim uncertainties of 0.5 to 5% in their thermal-diffusivity values, of less than 20 mK in their temperatures, and of about 0.3% in the densities. The specific-heat values used were calculated from the fundamental equation of state, which consists of the crossover model of van Pelt and Sengers [6] and the Tillner-Roth equation [7]. Since van Pelt and Sengers do not give the uncertainties in this quantity explicitly, but show a plot of regions where the deviation in c_p from the corresponding point calculated from the

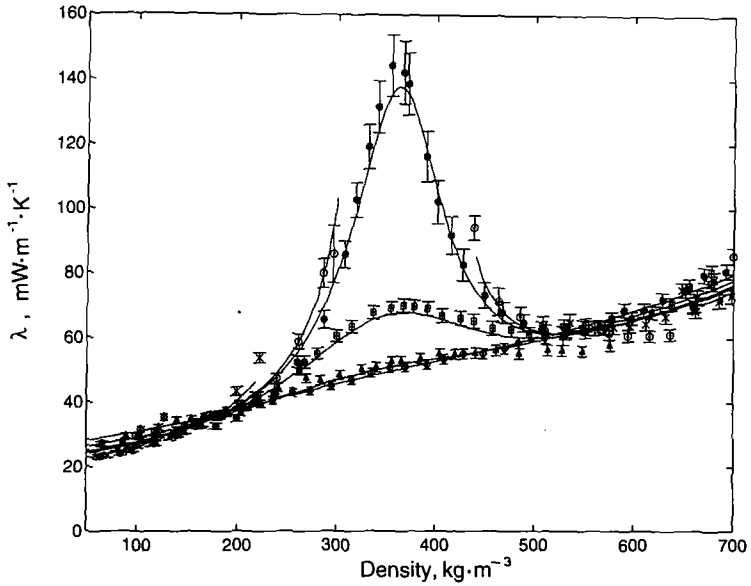

Fig. 9. The thermal conductivity of R152a in the critical region as a function of density. The symbols indicate values calculated from the experimental thermal-diffusivity data of Kruppa and Straub [37] along the various isotherms: (*) 367 K; (×) 382 K; (○) 386 K; (●) 387 K; (□) 390 K; (△) 405 K; (◇) 425 K. The solid curves represent the respective values calculated from all three terms in the representative Eq. (2) in this paper.

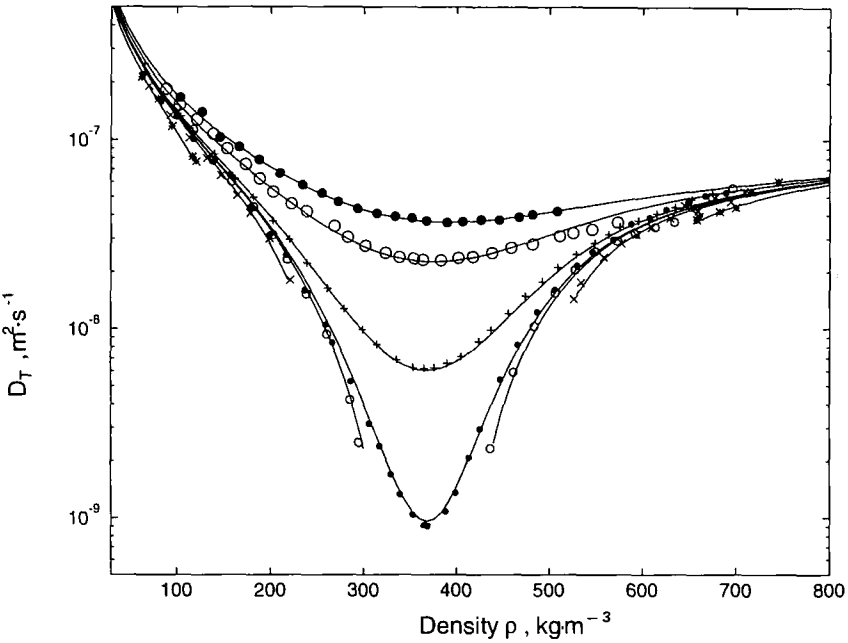

Fig. 10. The thermal diffusivity of R152a in the critical region as a function of density. The symbols indicate thermal-diffusivity data measured by Kruppa and Straub [37] along one of the respective isotherms: (*) 367 K; (×) 382 K; (○) 386 K; (●) 387 K; (+) 390 K; (○) 405 K; (●) 425 K. The solid curves represent the corresponding values calculated from Eqs. (2) and (19).

Tillner-Roth equation alone is less than 0.1, 0.5, and 1%, respectively, we estimate an error of 2% in the region where we apply this equation. (Tillner-Roth himself quotes an uncertainty of 2% in c_P for his equation of state [7].) Combined with the errors Kruppa and Straub quoted for the temperature and density, the total uncertainty in the c_P values, which were used to convert the D_T data into thermal conductivities, ranges from 2% away from the critical point to about 7% near the critical point on the lowest temperature supercritical isotherm (386.83 K). Adopting the value of 2% for the uncertainty in D_T and 0.3% for that in the density, the estimated uncertainties in λ are slightly higher, ranging from 2.8 to 7%.

The cutoff wavenumber q_D, the only adjustable constant in the expression for $\Delta_c D_T$, was determined from a least-squares fit of the values for λ thus deduced from the measurements of Kruppa and Straub to

$$\lambda = \bar{\lambda} + \Delta_c \lambda = \lambda_0(T) + \Delta_R \lambda(\rho) + \rho c_P \Delta_c D_T \tag{19}$$

where $\lambda_0(T)$ and $\Delta_R\lambda(\rho)$ are the background contributions introduced in Eq. (2) (Section 2) and where $\Delta_c D_T$ is given by Eq. (13). For the fitting procedure all the data in the one-phase region taken along the seven isotherms except for those with densities greater than 600 kg · m^{-3} and two data points of the 386.06 K isotherm closest to the phase boundary were used. In this way data that are suspected of having larger errors due to lower light-scattering intensities are excluded from the fit. Thus we found a value of $q_D^{-1} = 4.37$ Å, somewhat larger than reported for other fluids [8–11, 30, 50–55]. The values of all constants in the equations for the critical enhancements of the transport properties are given in Table V.

In Fig. 9, the thermal-conductivity data calculated from the thermal-diffusivity data of Kruppa and Straub as well as the values calculated from the crossover theory are displayed graphically. The absolute mean error (AME) for the complete set of Kruppa and Straub is about 3%, the maximum error being ±14%. In Figs. 10 and 11, comparisons between their thermal-diffusivity data along the seven isotherms, the phase boundary,

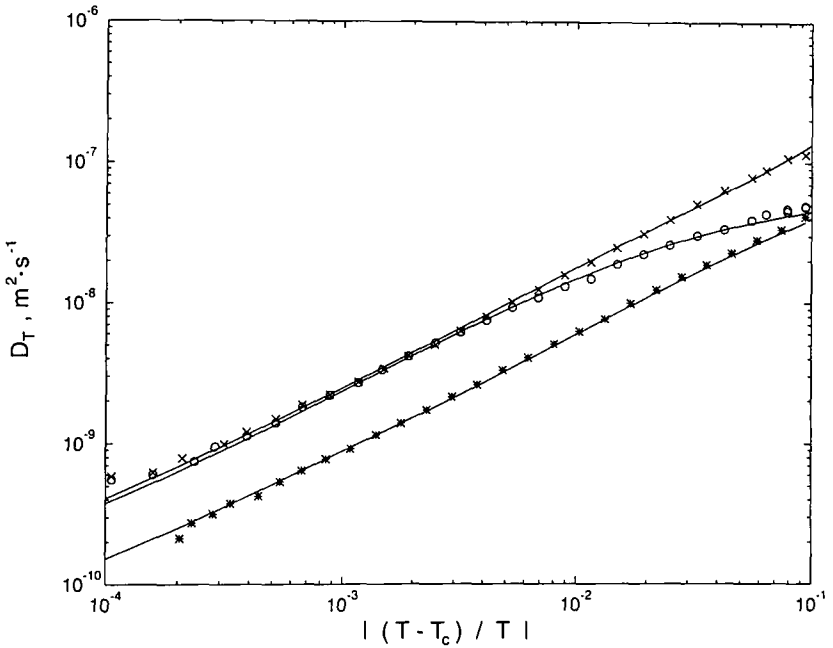

Fig. 11. The thermal diffusivity of R152a on the critical isochore and on the phase boundary as functions of the reduced temperature. The symbols indicate experimental values obtained by Kruppa and Straub [37]: (*) critical isochore; (○) liquid phase; (×) vapor phase. The solid curves represent the corresponding values calculated from the crossover model for transport properties.

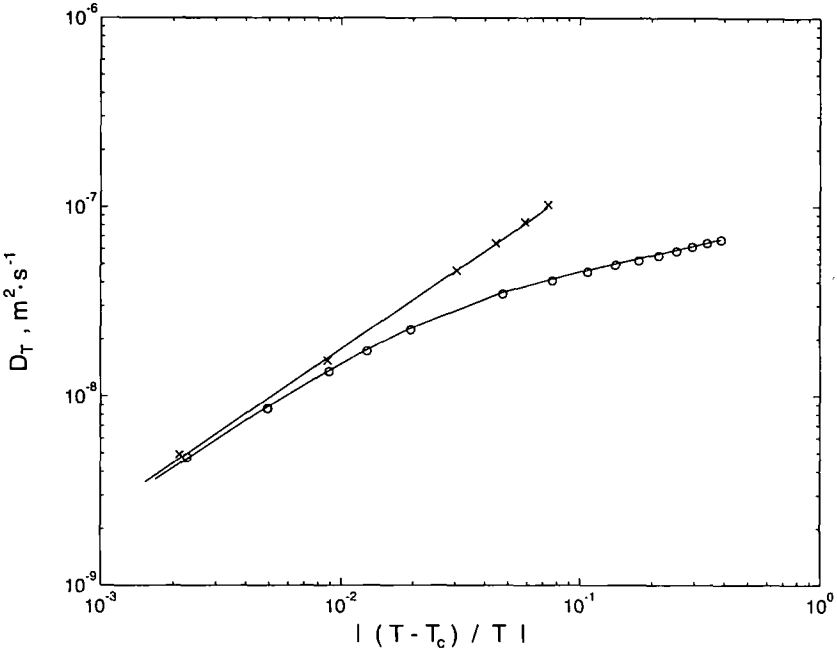

Fig. 12. The thermal diffusivity of R152a along the phase boundary. The symbols indicate the thermal diffusivity data measured by Leipertz and Kraft [36]: (○) liquid phase; (×) vapor phase. The solid lines represent values calculated from the crossover model for transport properties.

and along the critical isochore, respectively, are shown. The agreement between theoretical and experimental data is satisfactory. The experimental thermal-diffusivity data measured by Kraft and Leipertz along the phase boundary are plotted together with the corresponding theoretical values in Fig. 12. After having shifted their temperatures by +0.23 K, which seems justifiable since they do not quote a value for T_c along with their data, the agreement is quite good.

As mentioned in Section 3, no data are available for the viscosity in the critical region.

6. RESULTS

The viscosity η can be calculated from Eq. (1), where the dilute-gas term $\eta_0(T)$ is represented by Eq. (4) and where the equation for the excess contribution $\Delta_R\eta(\rho)$ is given by Eq. (6). The critical enhancement $\Delta_c\eta$ can

be estimated from Eq. (14). The thermal conductivity λ can be calculated from Eq. (2), where the dilute-gas term $\lambda_0(T)$ is represented by Eq. (7), the equation for the excess contribution $\Delta_R\lambda(\rho)$ is given by Eq. (8), while the critical enhancement $\Delta_c\lambda$ can be calculated from Eqs. (13) and (10). The correlating equations for both transport properties are valid for temperatures ranging from 240 to 440 K, for pressures up to 20 MPa, and for densities up to 1050 $kg \cdot m^{-3}$.

Values for the viscosity and the thermal conductivity of R152a, as calculated from Eqs. (1) and (2) are listed in Tables VI, VII, and VIII. Specifically, Table VI gives the transport properties at saturation as a function of temperature, where a single prime refers to the saturated liquid and a double prime to the saturated vapor. Values calculated for the transport properties at $P = 0.1$ MPa, indicated by the subscript 0.1, are also presented in Table VI. Values calculated for the transport properties at selected temperatures and pressures are listed in Tables VII and VIII.

The region where the critical enhancement of the viscosity exceeds 1% of the total viscosity can be approximated by a trapezoid with the corners

$$\begin{aligned} &386\ \text{K}, 255\ \text{kg} \cdot \text{m}^{-3}, \quad \text{and} \quad 386\ \text{K}, 455\ \text{kg} \cdot \text{m}^{-3} \\ &390\ \text{K}, 300\ \text{kg} \cdot \text{m}^{-3}, \quad \text{and} \quad 390\ \text{K}, 400\ \text{kg} \cdot \text{m}^{-3} \end{aligned} \tag{20}$$

Similarly the region where the critical enhancement of the thermal conductivity $\Delta_c\lambda$ exceeds 3% of the total quantity λ is bounded approximately by

$$\begin{aligned} &360\ \text{K}, 80\ \text{kg} \cdot \text{m}^{-3}, \quad \text{and} \quad 370\ \text{K}, 640\ \text{kg} \cdot \text{m}^{-3} \\ &440\ \text{K}, 160\ \text{kg} \cdot \text{m}^{-3}, \quad \text{and} \quad 440\ \text{K}, 540\ \text{kg} \cdot \text{m}^{-3} \end{aligned} \tag{21}$$

Actually, a critical-enhancement contribution to the thermal conductivity extends to higher temperatures beyond 440 K, but 440 K is the maximum temperature of validity of the present correlation.

The overall uncertainty in the background correlation for the viscosity is estimated as $\pm 3\%$; that for the thermal conductivity, as $\pm 5\%$.

7. CONCLUSION

Based on a critical review of the available data, equations for the viscosity and thermal conductivity of R152a were developed that are valid in a wide range of temperatures and pressures, including the critical region. Analysis and evaluation of the experimental data showed that, for the viscosity, further precise measurements are needed, especially in the subcritical vapor phase and in the near and extended critical region. In the

Table VI. Thermophysical Properties at Saturation and at $P = 0.1$ MPa

T (K)	P_{sat} (MPa)	ρ' (kg · m^{-3})	ρ'' (kg · m^{-3})	η' (μPa · s)	η'' (μPa · s)	$\eta_{0.1}$ (μPa · s)	λ' (mW · m^{-1} · K^{-1})	λ'' (mW · m^{-1} · K^{-1})	$\lambda_{0.1}$ (mW · m^{-1} · K^{-1})
240	0.066420	1029.6	2.2736	364.8	8.097	365.1	128.9	8.417	128.9
242	0.073086	1025.5	2.4868	347.3	8.174	347.5	127.9	8.611	127.9
244	0.080276	1021.4	2.7157	332.0	8.251	332.2	126.8	8.806	126.8
246	0.088018	1017.3	2.9609	318.6	8.329	318.6	125.8	9.001	125.8
248	0.096342	1013.2	3.2233	306.5	8.406	306.6	124.8	9.195	124.8
250	0.10528	1009.0	3.5038	295.7	8.473	8.483	123.8	9.496	9.390
252	0.11486	1004.8	3.8032	285.8	8.549	8.559	122.8	9.700	9.585
254	0.12511	1000.6	4.1225	276.7	8.625	8.636	121.8	9.905	9.779
256	0.13608	996.36	4.4625	268.4	8.701	8.713	120.8	10.11	9.974
258	0.14778	992.10	4.8243	260.6	8.777	8.789	119.8	10.32	10.17
260	0.16026	987.81	5.2089	253.3	8.852	8.866	118.8	10.52	10.36
262	0.17355	983.49	5.6172	246.5	8.928	8.942	117.8	10.73	10.56
264	0.18768	979.14	6.0503	240.0	9.003	9.018	116.8	10.94	10.75
266	0.20269	974.76	6.5094	233.9	9.079	9.094	115.9	11.15	10.95
268	0.21862	970.35	6.9956	228.1	9.154	9.170	114.9	11.36	11.14
270	0.23551	965.90	7.5100	222.6	9.230	9.245	114.0	11.57	11.34
272	0.25338	961.42	8.0539	217.3	9.305	9.321	113.0	11.79	11.53
274	0.27229	956.91	8.6285	212.2	9.380	9.396	112.1	12.00	11.73
276	0.29227	952.37	9.2352	207.3	9.456	9.472	111.1	12.22	11.92
278	0.31335	947.78	9.8752	202.7	9.531	9.547	110.2	12.43	12.12
280	0.33558	943.16	10.550	198.1	9.606	9.622	109.2	12.65	12.31
282	0.35901	938.50	11.261	193.7	9.682	9.697	108.3	12.87	12.50

284	0.38366	933.80	12.010	189.5	9.758	9.772	107.4	13.09	12.70
286	0.40959	929.05	12.798	185.4	9.833	9.847	106.5	13.32	12.89
288	0.43683	924.26	13.627	181.4	9.909	9.921	105.6	13.54	13.09
290	0.46543	919.43	14.499	177.5	9.985	9.996	104.6	13.77	13.28
292	0.49544	914.54	15.416	173.7	10.06	10.07	103.7	14.00	13.48
294	0.52688	909.61	16.379	170.0	10.14	10.14	102.8	14.23	13.67
296	0.55982	904.63	17.390	166.4	10.22	10.22	101.9	14.46	13.87
298	0.59429	899.60	18.452	162.9	10.29	10.29	101.0	14.70	14.06
300	0.63035	894.51	19.567	159.4	10.37	10.37	100.1	14.94	14.26
302	0.66803	889.36	20.737	156.1	10.45	10.44	99.25	15.18	14.45
304	0.70738	884.15	21.964	152.7	10.53	10.51	98.36	15.42	14.65
306	0.74846	878.88	23.252	149.5	10.61	10.59	97.48	15.67	14.84
308	0.79130	873.54	24.602	146.3	10.69	10.66	96.59	15.92	15.04
310	0.83596	868.14	26.018	143.2	10.77	10.73	95.71	16.17	15.23
312	0.88249	862.66	27.503	140.1	10.85	10.81	94.84	16.43	15.42
314	0.93093	857.11	29.060	137.1	10.94	10.88	93.96	16.70	15.62
316	0.98134	851.48	30.693	134.1	11.02	10.95	93.08	16.97	15.81
318	1.0338	845.77	32.406	131.2	11.11	11.03	92.21	17.24	16.01
320	1.0883	839.97	34.202	128.3	11.20	11.10	91.34	17.52	16.20
322	1.1449	834.08	36.086	125.5	11.29	11.17	90.46	17.80	16.40
324	1.2037	828.10	38.063	122.7	11.38	11.24	89.59	18.09	16.59
326	1.2647	822.01	40.137	119.9	11.48	11.32	88.72	18.39	16.79
328	1.3280	815.82	42.315	117.2	11.58	11.39	87.85	18.70	16.98
330	1.3937	809.51	44.602	114.5	11.68	11.46	86.97	19.01	17.18
332	1.4617	803.09	47.005	111.8	11.78	11.53	86.10	19.33	17.37
334	1.5323	796.53	49.532	109.2	11.89	11.60	85.22	19.67	17.57
336	1.6053	789.85	52.189	106.6	12.00	11.68	84.35	20.01	17.76
338	1.6809	783.02	54.986	104.0	12.11	11.75	83.47	20.37	17.95

Table VI. *(Continued)*

T (K)	P_{sat} (MPa)	ρ' (kg·m^{-3})	ρ'' (kg·m^{-3})	η' (μPa·s)	η'' (μPa·s)	$\eta_{0.1}$ (μPa·s)	λ' (mW·m^{-1}·K^{-1})	λ'' (mW·m^{-1}·K^{-1})	$\lambda_{0.1}$ (mW·m^{-1}·K^{-1})
340	1.7592	776.03	57.933	101.4	12.23	11.82	82.58	20.74	18.15
342	1.8401	768.88	61.039	98.89	12.36	11.89	81.70	21.12	18.34
344	1.9239	761.55	64.318	96.38	12.49	11.96	80.81	21.52	18.54
346	2.0105	754.04	67.783	93.88	12.63	12.03	79.91	21.94	18.73
348	2.1000	746.31	71.449	91.40	12.77	12.10	79.01	22.39	18.93
350	2.1924	738.36	75.333	88.94	12.93	12.17	78.10	22.85	19.12
352	2.2880	730.17	79.455	86.48	13.09	12.25	77.19	23.35	19.32
354	2.3867	721.72	83.838	84.04	13.27	12.32	76.26	23.88	19.51
356	2.4886	712.97	88.509	81.61	13.45	12.39	75.33	24.44	19.71
358	2.5938	703.90	93.499	79.18	13.65	12.46	74.39	25.04	19.90
360	2.7024	694.46	98.845	76.75	13.87	12.53	73.43	25.70	20.10
362	2.8145	684.62	104.59	74.31	14.11	12.60	72.46	26.41	20.29
364	2.9301	674.32	110.79	71.87	14.37	12.67	71.47	27.19	20.49
366	3.0490	662.15	117.33	69.11	14.65	12.74	70.36	28.07	20.68
368	3.1719	650.90	124.84	66.69	14.98	12.81	69.37	29.02	20.87
370	3.2990	639.00	133.01	64.24	15.34	12.88	68.36	30.09	21.07
372	3.4303	626.29	142.01	61.75	15.75	12.95	67.33	31.33	21.26
374	3.5660	612.55	152.01	59.21	16.22	13.02	66.29	32.80	21.46
376	3.7063	597.47	163.32	56.56	16.77	13.09	65.24	34.59	21.65
378	3.8512	580.54	176.40	53.78	17.42	13.15	64.22	36.86	21.85
380	4.0011	560.92	192.01	50.77	18.25	13.22	63.33	39.98	22.04
382	4.1563	536.95	211.70	47.39	19.34	13.29	62.93	44.74	22.24
384	4.3171	504.51	239.35	43.29	21.01	13.36	64.51	53.93	22.43
386	4.4846	441.81	296.01	36.91	25.20	13.43	85.58	98.39	22.63

Table VII. Viscosity of R152a (μPa·s)

P (MPa)	T(K) 240	250	260	270	280	290	300	310	320	330	340	350	360	370	380	390	400	410	420	430	440
0.1	365.1	8.483	8.866	9.245	9.622	9.996	10.37	10.73	11.10	11.46	11.82	12.17	12.53	12.88	13.22	13.57	13.91	14.25	14.58	14.92	15.25
0.5	368.4	297.6	254.5	223.4	198.6	177.6	10.36	10.72	11.09	11.45	11.81	12.16	12.51	12.86	13.21	13.55	13.89	14.23	14.57	14.90	15.23
1.0	372.6	300.1	256.5	224.9	200.0	178.9	160.4	143.6	11.17	11.52	11.87	12.21	12.56	12.90	13.25	13.59	13.92	14.26	14.59	14.92	15.25
1.5	377.0	302.6	258.2	226.5	201.4	180.2	161.7	145.0	129.5	114.8	12.05	12.37	12.69	13.02	13.35	13.68	14.01	14.33	14.66	14.99	15.31
2.0	381.5	305.2	260.1	228.0	202.7	181.5	163.0	146.3	130.9	116.3	102.3	12.70	12.96	13.25	13.54	13.85	14.16	14.47	14.79	15.10	15.41
2.5	386.1	307.8	261.9	229.6	204.1	182.9	164.3	147.6	132.2	117.8	103.9	90.17	13.50	13.65	13.87	14.13	14.40	14.69	14.98	15.27	15.57
3.0	390.8	310.4	263.8	231.1	205.5	184.2	165.6	148.9	133.6	119.2	105.5	92.09	78.24	14.42	14.42	14.56	14.76	14.99	15.25	15.51	15.79
3.5	395.7	313.1	265.7	232.7	206.9	185.5	166.8	150.2	134.9	120.7	107.1	93.90	80.56	65.89	15.42	15.25	15.29	15.43	15.62	15.84	16.07
4.0	400.7	315.8	267.7	234.2	208.3	186.8	168.1	151.4	136.2	122.0	108.6	95.63	82.69	69.03	18.23	16.42	16.09	16.05	16.12	16.26	16.44
4.5	405.9	318.6	269.6	235.8	209.7	188.0	169.4	152.7	137.5	123.4	110.1	97.29	84.68	71.71	56.73	19.02	17.36	16.92	16.80	16.81	16.91
5.0	411.3	321.4	271.6	237.4	211.0	189.3	170.6	153.9	138.8	124.7	111.5	98.89	86.55	74.10	60.62	40.29	19.66	18.20	17.71	17.53	17.50
5.5	416.9	324.3	273.6	239.0	212.4	190.6	171.8	155.2	140.0	126.0	112.9	100.4	88.32	76.28	63.73	48.83	25.35	20.21	18.96	18.45	18.23
6.0	422.7	327.2	275.6	240.6	213.8	191.9	173.1	156.4	141.3	127.3	114.3	101.9	90.01	78.30	66.39	53.40	36.29	23.57	20.71	19.64	19.13
6.5	428.6	330.2	277.6	242.2	215.2	193.2	174.3	157.6	142.5	128.6	115.6	103.4	91.63	80.19	68.76	56.84	43.26	29.00	23.17	21.17	20.25
7.0	434.8	333.3	279.6	243.8	216.6	194.4	175.5	158.8	143.7	129.8	116.9	104.8	93.20	81.98	70.93	59.71	47.80	35.09	26.54	23.14	21.61
7.5	441.2	336.4	281.7	245.4	218.0	195.7	176.7	160.0	144.9	131.1	118.2	106.2	94.71	83.68	72.93	62.23	51.30	40.05	30.58	25.58	23.26
8.0	447.9	339.6	283.8	247.0	219.4	197.0	177.9	161.2	146.1	132.3	119.5	107.5	96.17	85.31	74.80	64.50	54.23	43.96	34.65	28.44	25.19
8.5	454.9	342.8	285.9	248.6	220.8	198.3	179.1	162.3	147.3	133.5	120.8	108.8	97.59	86.88	76.58	66.58	56.78	47.19	38.31	31.49	27.37
9.0	462.1	346.1	288.0	250.3	222.2	199.5	180.3	163.5	148.4	134.7	122.0	110.1	98.97	88.38	78.26	68.51	59.08	49.97	41.51	34.51	29.73
9.5	469.7	349.5	290.2	252.0	223.6	200.8	181.5	164.7	149.6	135.9	123.2	111.4	100.3	89.84	79.87	70.33	61.18	52.44	44.32	37.35	31.14
10.0	477.6	352.9	292.4	253.6	225.0	202.1	182.7	165.8	150.7	137.0	124.4	112.6	101.6	91.26	81.42	72.05	63.13	54.67	46.83	39.97	34.53
11.0	494.4	360.1	296.9	257.0	227.8	204.6	185.1	168.1	153.0	139.3	126.7	115.1	104.2	93.97	84.35	75.26	66.69	58.64	51.21	44.58	39.00
12.0	513.0	367.6	301.5	260.4	230.7	207.1	187.5	170.4	155.2	141.5	129.0	117.4	106.6	96.55	87.10	78.22	69.90	62.13	54.98	48.55	42.98
13.0	—	375.5	306.2	263.9	223.6	209.7	189.8	172.7	157.5	143.7	131.2	119.7	109.0	99.02	89.71	80.99	72.85	65.29	58.34	52.07	46.55
14.0	—	383.8	311.1	267.4	236.5	212.2	192.2	174.9	159.6	145.9	133.4	121.9	111.3	101.4	92.19	83.60	75.61	68.20	61.40	55.24	49.77
15.0	—	392.6	316.1	271.0	239.4	214.8	194.5	177.1	161.8	148.1	135.6	124.1	113.5	103.7	94.57	86.08	78.20	70.92	64.23	58.16	52.73
16.0	—	402.0	321.3	274.7	242.3	217.4	196.9	179.3	163.9	150.2	137.7	126.2	115.7	105.9	96.86	88.46	80.67	73.47	66.87	60.87	55.48
17.0	—	411.9	326.7	278.5	245.3	219.9	199.2	181.5	166.1	152.2	139.7	128.3	117.8	108.1	99.07	90.74	83.02	75.90	69.36	63.41	58.05
18.0	—	422.5	332.3	282.3	248.3	222.5	201.5	183.7	168.2	154.3	141.8	130.3	119.9	110.2	101.2	92.93	85.27	78.21	71.73	65.82	60.48
19.0	—	433.7	338.1	286.2	251.4	225.7	203.9	185.9	170.3	156.3	143.8	132.4	121.9	112.3	103.3	95.06	87.45	80.43	73.98	68.10	62.78
20.0	—	445.9	344.1	290.2	254.5	227.7	206.2	188.1	172.3	158.4	145.8	134.3	123.9	114.2	105.3	97.12	89.54	82.56	76.15	70.29	64.98

Table VIII. Thermal Conductivity of R152a ($mW \cdot m^{-1} \cdot K^{-1}$)

P	T(K)																				
(MPa)	240	250	260	270	280	290	300	310	320	330	340	350	360	370	380	390	400	410	420	430	440
0.1	128.9	9.39	10.36	11.34	12.31	13.28	14.26	15.23	16.20	17.18	18.15	19.12	20.10	21.06	22.04	23.02	23.99	24.96	25.94	26.91	27.88
0.5	129.1	124.0	119.0	114.1	109.4	104.7	14.74	15.69	16.63	17.58	18.54	19.50	20.46	21.42	22.38	23.34	24.30	25.27	26.23	27.20	28.16
1.0	129.4	124.3	119.3	114.4	109.7	105.0	100.4	95.86	17.33	18.19	19.08	20.00	20.92	21.85	22.79	23.73	24.68	25.62	26.57	27.53	28.48
1.5	129.7	124.5	119.6	114.8	110.0	105.4	100.8	96.31	91.76	87.10	19.96	20.72	21.56	22.42	23.31	24.22	25.13	26.05	26.98	27.91	28.85
2.0	129.9	124.8	119.9	115.1	110.4	105.8	101.2	96.75	92.25	87.68	82.92	21.99	22.51	23.22	24.00	24.83	25.69	26.56	27.45	28.36	29.27
2.5	130.2	125.1	120.2	115.4	110.7	106.1	101.6	97.19	92.74	88.24	83.59	78.63	24.29	24.44	24.96	25.63	26.39	27.19	28.02	28.88	29.75
3.0	130.4	125.4	120.5	115.7	111.0	106.5	102.0	97.61	93.22	88.79	84.24	79.44	74.10	26.75	26.43	26.74	27.30	27.97	28.71	29.50	30.31
3.5	130.7	125.6	120.7	116.0	111.4	106.8	102.4	98.03	93.68	89.32	84.86	80.21	75.13	69.07	29.14	28.40	28.52	28.96	29.55	30.23	30.97
4.0	131.0	125.9	121.0	116.3	111.7	107.2	102.8	98.44	94.14	89.83	85.46	80.93	76.07	70.50	39.89	31.25	30.28	30.25	30.59	31.11	31.73
4.5	131.2	126.2	121.3	116.6	112.0	107.5	103.1	98.84	94.59	90.34	86.04	81.63	76.95	71.74	65.25	38.26	33.01	32.01	31.91	32.17	32.63
5.0	131.5	126.4	121.6	116.9	112.3	107.9	103.5	99.24	95.03	90.83	86.61	82.29	77.77	72.85	67.03	60.69	37.96	34.50	33.60	33.47	33.70
5.5	131.7	126.7	121.9	117.2	112.6	108.2	103.9	99.63	95.46	91.31	87.15	82.93	78.54	73.86	68.52	61.83	48.91	38.20	35.82	35.07	34.95
6.0	132.0	127.0	122.1	117.5	112.9	108.5	104.2	100.0	95.88	91.78	87.68	83.54	79.28	74.79	69.80	63.91	56.37	43.73	38.72	37.02	36.43
6.5	132.2	127.2	122.4	117.8	113.2	108.9	104.6	100.4	96.30	92.24	88.20	84.13	79.98	75.66	70.95	65.61	59.06	50.04	42.21	39.39	38.16
7.0	132.5	127.5	122.7	118.1	113.6	109.2	104.9	100.8	96.71	92.69	88.71	84.71	80.65	76.45	71.99	67.06	61.31	54.29	46.60	42.16	40.15
7.5	132.7	127.8	123.0	118.3	113.9	109.5	105.3	101.2	97.11	93.14	89.20	85.26	81.29	77.22	72.95	68.33	63.15	57.15	50.47	45.22	42.37
8.0	133.0	128.0	123.2	118.6	114.2	109.8	105.6	101.5	97.51	93.57	89.68	85.80	81.91	77.94	73.84	69.47	64.71	59.40	53.58	48.28	44.77
8.5	133.2	128.3	123.5	118.9	114.5	110.1	106.0	101.9	97.90	94.00	90.15	86.33	82.51	78.64	74.67	70.50	66.06	61.25	56.08	51.07	47.22
9.0	133.4	128.5	123.8	119.2	114.8	110.5	106.3	102.2	98.29	94.42	90.61	86.84	83.09	79.31	75.45	71.47	67.28	62.83	58.15	53.51	49.58
9.5	133.7	128.8	124.0	119.5	115.0	110.8	106.6	102.6	98.67	94.83	91.06	87.34	83.65	79.95	76.20	72.36	68.38	64.22	59.91	55.61	51.77
10.0	133.9	129.0	124.3	119.7	115.3	111.1	107.0	102.9	99.04	95.24	91.50	87.83	84.19	80.56	76.91	73.20	69.39	65.47	61.45	57.45	53.75
11.0	134.4	129.5	124.8	120.3	115.9	111.7	107.6	103.6	99.78	96.03	92.37	88.77	85.24	81.73	78.25	74.75	71.21	67.64	64.05	60.51	57.15
12.0	134.9	130.0	125.3	120.8	116.5	112.3	108.2	104.3	100.5	96.80	93.20	89.68	86.23	82.84	79.48	76.15	72.83	69.51	66.22	63.01	59.94
13.0	—	130.5	125.9	121.4	117.1	112.9	108.9	105.0	101.2	97.55	94.01	90.55	87.18	83.88	80.64	77.44	74.29	71.18	68.10	65.13	62.29
14.0	—	131.0	126.4	121.9	117.6	113.5	109.5	105.6	101.9	98.28	94.79	91.39	88.09	84.87	81.73	78.65	75.63	72.68	69.79	67.01	64.35
15.0	—	131.5	126.9	122.4	118.2	114.0	110.1	106.2	102.6	98.99	95.55	92.21	88.97	85.82	82.76	79.78	76.87	74.05	71.31	68.67	66.16
16.0	—	132.0	127.4	122.9	118.7	114.6	110.7	106.9	103.2	99.69	96.29	93.00	89.81	86.73	83.74	80.84	78.03	75.31	72.69	70.18	67.79
17.0	—	132.4	127.9	123.5	119.2	115.2	111.2	107.5	103.9	100.4	97.01	93.76	90.63	87.60	84.68	81.86	79.13	76.50	73.97	71.56	69.28
18.0	—	132.9	128.3	124.0	119.8	115.7	111.8	108.1	104.5	101.0	97.71	94.51	91.42	88.45	85.58	82.82	80.16	77.61	75.17	72.84	70.64
19.0	—	133.4	128.8	124.5	120.3	116.3	112.4	108.7	105.1	101.7	98.40	95.23	92.19	89.26	86.45	83.75	81.15	78.67	76.30	74.04	71.92
20.0	—	133.8	129.3	125.0	120.8	116.8	113.0	109.3	105.7	102.3	99.07	95.94	92.94	90.05	87.29	84.63	82.10	79.67	77.36	75.17	73.11

case of the thermal conductivity of R152a we also need more precise measurements in the subcritical vapor phase, even at atmospheric pressure, as well as in the near and extended critical region.

ACKNOWLEDGMENTS

The authors are indebted to A. van Pelt and J. Luettmer-Strathmann for valuable discussions and for assistance in evaluating the critical enhancements. We are indebted to M. J. Assael, P. S. van der Gulik, K. Kraft and A. Leipertz, B. Kruppa and J. Straub, and C. A. Nieto de Castro for providing us with experimental data, partly prior to publication. R. Tillner-Roth supplied us with a computer program for his equation of state for R152a, and A. Laesecke with some literature data sets. V. C. Weiss' stay at the University of Maryland at College Park was part of an exchange program between the University of Maryland and the University of Bremen. V.C.W. would like to thank both institutions as well as the German Academic Exchange Service (DAAD) for granting a partial scholarship for the time of his stay. The research at the University of Stuttgart was supported by the German Bundesminister für Forschung und Technologie under Grant 0329255A. The research at the University of Maryland was supported by the Division of Chemical Sciences of the Office of Basic Energy Sciences of the U.S. Department of Energy under Grant DE-FG02-95ER14509. The research was carried out under the auspices of the Subcommittee on Transport Properties of Commission I.2 of the International Union of Pure and Applied Chemistry.

REFERENCES

1. D. J. Wuebbles, *Int. J. Refrig.* **17**:7 (1994).
2. R. Krauss and K. Stephan, *Proc. Joint Meet. IIR Comm. B1, B2, E1, E2* (Padova 1994), p. 363.
3. R. Krauss and K. Stephan, *DKV-Tagungsbericht* (Bonn 1994) **21**:159 (1994).
4. J. V. Sengers, *Int. J. Thermophys.* **6**:203 (1985).
5. J. V. Sengers, in *Supercritical Fluids*, E. Kiran and J. M. H. Levelt Sengers, eds. (Kluwer, Dordrecht, 1994), p. 231.
6. A. van Pelt and J. V. Sengers, *J. Supercrit. Fluids* **8**:81 (1995).
7. R. Tillner-Roth, *Int. J. Thermophys.* **16**:91 (1995).
8. V. Vesovic, W. A. Wakeham, G. A. Olchowy, J. V. Sengers, J. T. R. Watson, and J. Millat, *J. Phys. Chem. Ref. Data* **19**:763 (1990).
9. R. Krauss, J. Luettmer-Strathmann, J. V. Sengers, and K. Stephan, *Int. J. Thermophys.* **14**:951 (1993).
10. S. Hendl, J. Millat, E. Vogel, V. Vesovic, W. A. Wakeham, J. Luettmer-Strathmann, J. V. Sengers, and M. J. Assael, *Int. J. Thermophys.* **15**:1 (1994).
11. V. Vesovic, W. A. Wakeham, J. Luettmer-Strathmann, J. V. Sengers, J. Millat, E. Vogel, and M. J. Assael, *Int. J. Thermophys.* **15**:33 (1994).

12. G. A. Olchowy and J. V. Sengers, *Phys. Rev. Lett.* **61**:15 (1988).
13. M. J. Assael, K. Polimatidou, and W. A. Wakeham, *Int. J. Thermophys.* **15**:575 (1994).
14. F. Mayinger, *DFG-Forschungsvorhaben, Abschlussbericht* (1991).
15. M. Takahashi, C. Yokoyama, and S. Takahashi, *J. Chem. Eng. Data* **32**:98 (1987).
16. M. Takahashi, C. Yokoyama, and S. Takahashi, *Nippon Reito Kyokai Ronb. (Trans. JAR)* **4**:25 (1987).
17. P. S. van der Gulik, *Int. J. Thermophys.* **16**:867 (1995).
18. A. Arnemann and H. Kruse, *Proc. Int. Congr. Refrig.* (18) (Montréal, 1991), p. 379.
19. R. Heide and H. Lippold, *Proc. Meet. Int. Inst. Refrig. Comm. B2, E2, D1, D2/3*, (Dresden, 1990), p. 237.
20. A. Kumagai and S. Takahashi, *Int. J. Thermophys.* **12**:105 (1991).
21. A. Kumagai and S. Takahashi, *Proc. 8th Japan Symp. Thermophys. Prop.* (1987), p. 129.
22. I. N. Lapardin, *Izv. Vys. Ucheb. Zaved., Neft I Gaz* **25**:24 + 63 (1982).
23. W. H. Mears, R. F. Stahl, S. R. Orfeo, R. C. Shair, L. F. Kells, W. Thompson, and H. McCann, *Ind. Eng. Chem.* **47**:1449 (1955).
24. K. Nagoka, Y. Yamashita, Y. Tanaka, H. Kubota, and T. Makita, *J. Chem Eng. Japan* **19**:263 (1986).
25. T. W. Phillips and K. P. Murphy, *ASHRAE Trans.* **76**:146 (1970).
26. N. G. Sagaidakova, V. A. Rykov, and T. N. Tsuranova, *Kholod. Tekh.* **5**:59 (1990).
27. B. Schramm, J. Hauck, and L. Kern, *Ber. Bunsenges. Phys. Chem.* **96**:745 (1992).
28. M. Takahashi, C. Yokoyama, and S. Takahashi, *Proc. 7th Japan Symp. Thermophys. Prop.* (1986), p. 179.
29. E. Bich, J. Millat, and E. Vogel, *Wiss. Z. Wilh.-Pieck-Univ. Rostock* **26**:5 (1987).
30. A. Laesecke, R. Krauss, K. Stephan, and W. Wagner, *J. Phys. Chem. Ref. Data* **19**:1089 (1990).
31. R. Afshar and S. C. Saxena, *Int. J. Thermophys.* **1**:51 (1980).
32. M. J. Assael, L. Karagiannidis, and W. A. Wakeham, *Proc. ASME Winter Ann. Meet.* (New Orleans, 1993), p. 1.
33. A. N. Gurova, C. A. Mardolcar, and C. A. Nieto de Castro, submitted for publication (1994).
34. U. Hammerschmidt, *Int. J. Thermophys.* **16**:1203 (1995).
35. S. H. Kim, D. S. Kim, M. S. Kim, and S. T. Ro, *Int. J. Thermophys.* **14**:937 (1993).
36. K. Kraft and A. Leipertz, *Int. J. Thermophys.* **15**:791 (1994).
37. B. Kruppa and J. Straub, *Int. J. Thermophys.* (in press).
38. B. Taxis-Reischl, Thesis (University of Stuttgart, Stuttgart, 1994).
39. O. B. Tsvetkov, Yu. A. Laptev, and A. G. Asambaev, *Int. J. Thermophys.* (in press).
40. V. Z. Geller, G. V. Zaporozhan, and S. V. Ilyushenko, *Prom. Teplotekh.* **4**:77 (1982).
41. A. J. Grebenkov, Yu. G. Kotelevsky, V. V. Saplitza, O. V. Beljaeva, T. A. Zajatz, and B. D. Timofeev, *Proc. Joint Meet. IIR Comm. B1, B2, E1, E2* (Padova, 1994), p. 419.
42. U. Gross, Y. W. Song, and E. Hahne, *Fluid Phase Equil.* **76**:273 (1992).
43. U. Gross, Y. W. Song, and E. Hahne, *Int. J. Thermophys.* **13**:957 (1992).
44. M. Ibreighith, M. Fiebig, A. Leipertz, and G. Wu, *Fluid Phase Equil.* **80**:323 (1992).
45. P. M. Kesselman, V. V. Slyusarev, and I. A. Paramonov, *Inzh.-Fiz. Zh.* **32**:410 (1977).
46. W. Tauscher, *Wärme- und Stoffübertragung* **21**:140 (1986).
47. N. B. Vargaftik, L. P. Filippov, A. A. Tarzimanov, and E. E. Totskii, *Handbook of Thermal Conductivity of Liquids and Gases* (CRC Press, Boca Raton, FL, 1994).
48. J. Yata, M. Hori, T. Kurahashi, and T. Minamiyama, *Fluid Phase Equil.* **80**:287 (1992).
49. J. M. Yin, J. X. Guo, Z. Y. Zhao, L. C. Tan, and M. Zhao, *Fluid Phase Equil.* **30**:297 (1992).

50. R. Mostert, H. R. van den Berg, P. S. van der Gulik, and J. V. Sengers, *J. Chem. Phys.* **92**:5454 (1990).
51. R. A. Perkins, H. M. Roder, D. G. Friend, and C. A. Nieto de Castro, *Physica A* **173**:332 (1991).
52. R. A. Perkins, D. G. Friend, H. M. Roder, and C. A. Nieto de Castro, *Int. J. Thermophys.* **12**:965 (1991).
53. B. W. Tiesenga, E. P. Sakonidou, H. R. van den Berg, J. Luettmer-Strathmann, and J. V. Sengers, *J. Chem. Phys.* **101**:6944 (1994).
54. J. Luettmer-Strathmann and J. V. Sengers, *High Temp.-High Press.* (in press).
55. J. V. Sengers and J. Luettmer-Strathmann, in *Transport Properties of Fluids: Their Correlation, Prediction, and Estimation*, J. Millat, J. H. Dymond, and C. A. Nieto de Castro, eds. (Cambridge University Press), Chap. 6.
56. J. Luettmer-Strathmann, Ph.D. thesis (Institute for Physical Science and Technology, University of Maryland, College Park, 1994).
57. J. Luettmer-Strathmann, J. V. Sengers, and G. A. Olchowy, *J. Chem. Phys.* **103**:7482 (1995).
58. J. V. Sengers and J. M. H. Levelt Sengers, *Annu. Rev. Phys. Chem.* **37**:189 (1986).
59. R. F. Berg and M. R. Moldover, *J. Chem. Phys.* **89**:3694 (1988); **93**:1926 (1990).
60. J. C. Nieuwoudt and J. V. Sengers, *J. Chem. Phys.* **90**:457 (1989).
61. H. Hao, Ph. D. thesis (Department of Physics and Astronomy, University of Maryland, College Park, 1991).
62. B. Saager and J. Fischer, *Deutscher Kälte- und Klimaverein e.V.*, **16**:213 (1989).